NANO LETTERS

2003
Vol. 3, No. 9
1235−1238

Dependence of Optical Transition Energies on Structure for Single-Walled Carbon Nanotubes in Aqueous Suspension: An Empirical Kataura Plot

R. Bruce Weisman* and Sergei M. Bachilo

Department of Chemistry, Center for Nanoscale Science and Technology, and Center for Biological and Environmental Nanotechnology, Rice University, 6100 Main Street, Houston, Texas 77005

Received June 20, 2003; Revised Manuscript Received July 16, 2003

ABSTRACT

Spectrofluorimetric data for identified single-walled carbon nanotubes in aqueous SDS suspension have been accurately fit to empirical expressions. These are used to obtain the first model-independent prediction of first and second van Hove optical transitions as a function of structure for a wide range of semiconducting nanotubes. To allow for convenient use in support of spectral studies, the results are presented in equation, graphical, and tabular forms. These empirical findings differ significantly from Kataura plots computed using a simple tight-binding model. It is suggested that the empirically based results should be used in preference to conventional model-based predictions in spectroscopic nanotube research.

Introduction. One of the most intriguing and potentially useful features of single-walled carbon nanotubes (SWNT) is the sensitivity of their electronic and optical properties to physical structure.[1] A nanotube's diameter (d_t) and chiral angle (α) are uniquely related to a pair of integers (n, m) that describe its construction as a rolled-up graphene sheet. Except for very small diameter nanotubes, it is well known that structures for which $n - m$ is evenly divisible by 3 display metallic or semimetallic behavior, whereas other tubes only slightly different in structure have significant band gaps and show semiconducting behavior.[2] The quasi-one-dimensionality of SWNT gives sharp van Hove peaks in the density of electronic states. Optical properties of SWNT are dominated by transitions between corresponding van Hove peaks on opposite sides of the Fermi level. Knowing the energies of these E_{ii} van Hove transitions for specific (n, m) structures is important not only for absorption spectroscopy but also for the widely used method of resonance Raman spectroscopy in which matches between the incident or scattered light frequencies and van Hove transitions expose vibrational frequencies of selected nanotubes.[3−5] Nanotube investigators using optical methods are commonly guided by Kataura plots of E_{ii} transition energies vs tube diameter.[6] In the absence of detailed experimental data, these have been generated from parametrized model calculations of SWNT electronic structure.

Recent breakthroughs in SWNT spectroscopy now allow the construction of experimentally based Kataura-type plots. In semiconducting SWNT, the lowest-energy van Hove transition (at E_{11}) corresponds to absorption or luminescence directly across the band gap. Since the discovery of band-gap photoluminescence from isolated SWNT in bulk aqueous suspensions,[7] it has become possible to use spectrofluorimetry to explore the E_{11} and E_{22} transitions of a sizable number of semiconducting SWNT species. As was reported earlier from this laboratory, distinct first and second van Hove transition wavelengths have been observed for 33 semiconducting SWNT in a surfactant-suspended bulk sample, and each of these species has been assigned specific (n, m) structural indices.[8] Spectral transitions of six additional SWNT species were reported by Lebedkin et al. in a study of slightly larger diameter nanotubes in a different surfactant.[9] Because the identified nanotubes span a rather wide range of structures (ranging from 0.62 to 1.41 nm in diameter and from 3 to 28° in chiral angle), their measured transition frequencies can be used to anchor a robust empirical fitting function that allows extrapolation beyond the set of measured data. This provides the basis for a model-independent, empirically based Kataura plot that gives reliable predictions of optical transition frequencies versus (n, m) for semiconducting SWNT in aqueous surfactant suspensions. To enable easy use of the new predictions, we present them below as empirical functions of diameter and chiral angle, as graphs, and as tabulated values for more than 100 (n, m) structures.

* Corresponding author. E-mail: weisman@rice.edu.

10.1021/nl034428i CCC: $25.00
Published on Web 08/08/2003

Table 1. Structures and First and Second van Hove Optical Transitions[a] for Semiconducting SWNT Structures with Diameters between 0.48 and 2.0 nm

(*n*, *m*)	d_t (nm)	α (deg)	mod[b]	λ_{11} (nm)	$\bar{\nu}_{11}$ (cm^{-1})	E_{11} (eV)[c]	λ_{22} (nm)	$\bar{\nu}_{22}$ (cm^{-1})	E_{22} (eV)	(*n*, *m*)	d_t (nm)	α (deg)	mod[b]	λ_{11} (nm)	$\bar{\nu}_{11}$ (cm^{-1})	E_{11} (eV)[c]	λ_{22} (nm)	$\bar{\nu}_{22}$ (cm^{-1})	E_{22} (eV)
(4, 3)	0.483	25.28	1	700	14 283	1.771	398	25 147	3.118	(14, 12)	1.789	27.46	2	2059	4856	0.602	1181	8470	1.050
(5, 3)	0.556	21.79	2	720	13 884	1.721	522	19 147	2.374	(14, 13)	1.857	28.78	1	2141	4672	0.579	1208	8278	1.026
(5, 4)	0.620	26.33	1	835	11 974	1.485	483	20 697	2.566	(15, 1)	1.232	3.20	2	1426	7011	0.869	920	10 864	1.347
(6, 1)	0.521	7.59	2	653	15 323	1.900	632	15 828	1.962	(15, 2)	1.278	6.18	1	1622	6165	0.764	822	12 163	1.508
(6, 2)	0.572	13.90	1	894	11 183	1.387	418	23 900	2.963	(15, 4)	1.377	11.52	2	1589	6294	0.780	986	10 140	1.257
(6, 4)	0.692	23.41	2	873	11 452	1.420	578	17 312	2.146	(15, 5)	1.431	13.90	1	1752	5708	0.708	921	10 858	1.346
(6, 5)	0.757	27.00	1	976	10 244	1.270	566	17 667	2.190	(15, 7)	1.546	18.14	2	1779	5621	0.697	1064	9396	1.165
(7, 0)	0.556	0.00	1	962	10 397	1.289	395	25 318	3.139	(15, 8)	1.606	20.03	1	1907	5245	0.650	1035	9663	1.198
(7, 2)	0.650	12.22	2	802	12 468	1.546	626	15 977	1.981	(15, 10)	1.730	23.41	2	1987	5032	0.624	1156	8650	1.072
(7, 3)	0.706	17.00	1	992	10 083	1.250	505	19 820	2.457	(15, 11)	1.795	24.92	1	2086	4793	0.594	1158	8635	1.071
(7, 5)	0.829	24.50	2	1024	9768	1.211	645	15 496	1.921	(15, 13)	1.927	27.64	2	2207	4532	0.562	1259	7942	0.985
(7, 6)	0.895	27.46	1	1120	8930	1.107	648	15 441	1.914	(15, 14)	1.994	28.86	1	2287	4373	0.542	1288	7767	0.963
(8, 0)	0.635	0.00	2	776	12 886	1.598	660	15 146	1.878	(16, 0)	1.270	0.00	1	1623	6163	0.764	815	12 264	1.521
(8, 1)	0.678	5.82	1	1041	9603	1.191	471	21 226	2.632	(16, 2)	1.357	5.82	2	1561	6405	0.794	984	10 162	1.260
(8, 3)	0.782	15.30	2	952	10 508	1.303	665	15 029	1.863	(16, 3)	1.405	8.44	1	1746	5728	0.710	898	11 139	1.381
(8, 4)	0.840	19.11	1	1111	8997	1.116	589	16 981	2.105	(16, 5)	1.508	13.17	2	1732	5775	0.716	1055	9480	1.175
(8, 6)	0.966	25.28	2	1173	8525	1.057	718	13 928	1.727	(16, 6)	1.564	15.30	1	1884	5307	0.658	1000	9999	1.240
(8, 7)	1.032	27.80	1	1265	7908	0.981	728	13 727	1.702	(16, 8)	1.680	19.11	2	1925	5194	0.644	1138	8788	1.090
(9, 1)	0.757	5.21	2	912	10 964	1.359	691	14 466	1.794	(16, 9)	1.741	20.82	1	2046	4887	0.606	1115	8968	1.112
(9, 2)	0.806	9.83	1	1138	8790	1.090	551	18 155	2.251	(16, 11)	1.867	23.90	2	2134	4685	0.581	1233	8111	1.006
(9, 4)	0.916	17.48	2	1101	9086	1.126	722	13 843	1.716	(16, 12)	1.932	25.28	1	2231	4483	0.556	1238	8077	1.001
(9, 5)	0.976	20.63	1	1241	8055	0.999	672	14 883	1.845	(17, 0)	1.350	0.00	2	1552	6443	0.799	984	10 167	1.261
(9, 7)	1.103	25.87	2	1322	7567	0.938	793	12 610	1.563	(17, 1)	1.391	2.83	1	1744	5733	0.711	886	11 289	1.400
(9, 8)	1.170	28.05	1	1410	7093	0.879	809	12 362	1.533	(17, 3)	1.483	7.99	2	1699	5886	0.730	1050	9525	1.181
(10, 0)	0.794	0.00	1	1156	8652	1.073	537	18 606	2.307	(17, 4)	1.533	10.33	1	1873	5340	0.662	974	10 263	1.272
(10, 2)	0.884	8.95	2	1053	9493	1.177	737	13 574	1.683	(17, 6)	1.641	14.56	2	1875	5332	0.661	1125	8886	1.102
(10, 3)	0.936	12.73	1	1249	8006	0.993	632	15 834	1.963	(17, 7)	1.697	16.47	1	2019	4952	0.614	1079	9264	1.149
(10, 5)	1.050	19.11	2	1249	8006	0.993	788	12 695	1.574	(17, 9)	1.816	19.93	2	2072	4827	0.599	1212	8248	1.023
(10, 6)	1.111	21.79	1	1377	7262	0.900	754	13 262	1.644	(17, 10)	1.877	21.49	1	2188	4571	0.567	1195	8367	1.037
(10, 8)	1.240	26.33	2	1470	6805	0.844	869	11 502	1.426	(18, 1)	1.470	2.68	2	1682	5944	0.737	1048	9543	1.183
(10, 9)	1.307	28.26	1	1556	6428	0.797	889	11 248	1.395	(18, 2)	1.515	5.21	1	1868	5353	0.664	958	10 433	1.294
(11, 0)	0.873	0.00	2	1037	9644	1.196	745	13 431	1.665	(18, 4)	1.611	9.83	2	1838	5439	0.674	1118	8947	1.109
(11, 1)	0.916	4.31	1	1265	7906	0.980	610	16 388	2.032	(18, 5)	1.663	11.93	1	2003	4993	0.619	1052	9508	1.179
(11, 3)	1.014	11.74	2	1197	8353	1.036	793	12 617	1.564	(18, 7)	1.773	15.75	2	2020	4952	0.614	1197	8351	1.035
(11, 4)	1.068	14.92	1	1371	7295	0.904	712	14 036	1.740	(18, 8)	1.831	17.48	1	2156	4638	0.575	1159	8629	1.070
(11, 6)	1.186	20.36	2	1397	7157	0.887	858	11 661	1.446	(18, 10)	1.951	20.63	2	2218	4509	0.559	1288	7765	0.963
(11, 7)	1.248	22.69	1	1516	6597	0.818	836	11 968	1.484	(19, 0)	1.508	0.00	1	1867	5357	0.664	953	10 492	1.301
(11, 9)	1.377	26.70	2	1617	6183	0.767	947	10 564	1.310	(19, 2)	1.594	4.95	2	1816	5507	0.683	1114	8979	1.113
(11, 10)	1.444	28.43	1	1702	5877	0.729	969	10 320	1.280	(19, 3)	1.641	7.22	1	1994	5015	0.622	1033	9683	1.201
(12, 1)	0.995	3.96	2	1170	8549	1.060	799	12 516	1.552	(19, 5)	1.741	11.39	2	1979	5052	0.626	1187	8422	1.044
(12, 2)	1.041	7.59	1	1378	7255	0.900	686	14 575	1.807	(19, 6)	1.795	13.29	1	2135	4684	0.581	1130	8853	1.098
(12, 4)	1.145	13.90	2	1342	7452	0.924	855	11 693	1.450	(19, 8)	1.907	16.76	2	2164	4621	0.573	1271	7869	0.976
(12, 5)	1.201	16.63	1	1499	6670	0.827	793	12 605	1.563	(19, 9)	1.966	18.35	1	2295	4358	0.540	1238	8076	1.001
(12, 7)	1.321	21.36	2	1545	6473	0.803	930	10 751	1.333	(20, 0)	1.588	0.00	2	1808	5531	0.686	1113	8989	1.114
(12, 8)	1.384	23.41	1	1657	6036	0.748	917	10 910	1.353	(20, 1)	1.629	2.42	1	1990	5024	0.623	1023	9775	1.212
(12, 10)	1.515	27.00	2	1765	5666	0.703	1024	9763	1.210	(20, 3)	1.719	6.89	2	1952	5124	0.635	1181	8466	1.050
(12, 11)	1.582	28.56	1	1848	5412	0.671	1049	9535	1.182	(20, 4)	1.768	8.95	1	2122	4712	0.584	1108	9025	1.119
(13, 0)	1.032	0.00	1	1384	7228	0.896	677	14 770	1.831	(20, 6)	1.872	12.73	2	2121	4715	0.585	1258	7947	0.985
(13, 2)	1.120	7.05	2	1307	7651	0.949	858	11 661	1.446	(20, 7)	1.927	14.46	1	2269	4406	0.546	1208	8280	1.027
(13, 3)	1.170	10.16	1	1498	6676	0.828	764	13 095	1.624	(21, 1)	1.708	2.31	2	1938	5161	0.640	1178	8487	1.052
(13, 5)	1.278	15.61	2	1487	6723	0.834	922	10 843	1.344	(21, 2)	1.752	4.50	1	2116	4727	0.586	1095	9134	1.132
(13, 6)	1.336	17.99	1	1632	6127	0.760	874	11 441	1.419	(21, 4)	1.847	8.57	2	2090	4786	0.593	1250	8000	0.992
(13, 8)	1.457	22.17	2	1692	5909	0.733	1004	9956	1.234	(21, 5)	1.897	10.44	1	2253	4439	0.550	1184	8445	1.047
(13, 9)	1.521	24.01	1	1799	5558	0.689	997	10 027	1.243	(22, 0)	1.747	0.00	1	2114	4731	0.587	1090	9171	1.137
(13, 11)	1.652	27.25	2	1912	5230	0.648	1102	9071	1.125	(22, 2)	1.831	4.31	2	2070	4830	0.599	1245	8030	0.996
(13, 12)	1.719	28.68	1	1994	5015	0.622	1128	8862	1.099	(22, 3)	1.877	6.31	1	2243	4459	0.553	1168	8560	1.061
(14, 0)	1.111	0.00	2	1295	7721	0.957	859	11 640	1.443	(22, 5)	1.975	10.02	2	2229	4487	0.556	1320	7575	0.939
(14, 1)	1.153	3.42	1	1502	6660	0.826	748	13 364	1.657	(23, 0)	1.826	0.00	2	2064	4845	0.601	1244	8039	0.997
(14, 3)	1.248	9.52	2	1447	6910	0.857	920	10 867	1.347	(23, 1)	1.867	2.11	1	2238	4467	0.554	1160	8620	1.069
(14, 4)	1.300	12.22	1	1623	6162	0.764	842	11 875	1.472	(23, 3)	1.956	6.05	2	2205	4535	0.562	1314	7612	0.944
(14, 6)	1.411	17.00	2	1633	6123	0.759	992	10 078	1.250	(24, 1)	1.946	2.02	2	2193	4560	0.565	1311	7631	0.946
(14, 7)	1.470	19.11	1	1768	5655	0.701	955	10 476	1.299	(24, 2)	1.990	3.96	1	2365	4229	0.524	1231	8121	1.007
(14, 9)	1.594	22.85	2	1840	5435	0.674	1080	9261	1.148	(25, 0)	1.985	0.00	1	2362	4233	0.525	1228	8146	1.010
(14, 10)	1.658	24.50	1	1942	5148	0.638	1078	9279	1.150										

[a] As predicted by the empirical formulas in the text. [b] The value of mod($n - m$, 3). [c] E_{11} values represent emission peaks; to obtain absorption peak energies, add ca. 0.004 eV.

We suggest that these empirically based spectral predictions should be used in preference to model-based results because of their significantly higher accuracy.

Methods and Results. In our prior report, spectral transitions for 33 semiconducting species were fit semiquantitatively using simple functions of d_t and α to illustrate systematic structural trends. By allowing the exponents of cos(3α) and d_t to vary from their original values of 1 and 2, respectively, in the second term, we have now deduced expressions that reproduce the experimental data much more

closely. As before, different parameters apply according to whether mod($n - m$, 3) equals 1 or 2 (mod 1 or mod 2 species, respectively). The refined empirical functions for first and second van Hove transition frequencies are (for d_t in nm)

$$\bar{\nu}_{11}(\text{mod } 1) = \frac{1 \times 10^7 \text{ cm}^{-1}}{157.5 + 1066.9d_t} - 771 \text{ cm}^{-1}\frac{[\cos(3\alpha)]^{1.374}}{d_t^{2.272}} \quad (1a)$$

$$\bar{\nu}_{11}(\text{mod } 2) = \frac{1 \times 10^7 \text{ cm}^{-1}}{157.5 + 1066.9d_t} + 347 \text{ cm}^{-1}\frac{[\cos(3\alpha)]^{0.886}}{d_t^{2.129}} \quad (1b)$$

$$\bar{\nu}_{22}(\text{mod } 1) = \frac{1 \times 10^7 \text{ cm}^{-1}}{145.6 + 575.7d_t} + 1326 \text{ cm}^{-1}\frac{[\cos(3\alpha)]^{0.828}}{d_t^{1.809}} \quad (2a)$$

$$\bar{\nu}_{22}(\text{mod } 2) = \frac{1 \times 10^7 \text{ cm}^{-1}}{145.6 + 575.7d_t} - 1421 \text{ cm}^{-1}\frac{[\cos(3\alpha)]^{1.110}}{d_t^{2.497}} \quad (2b)$$

These expressions mimic our experimental findings with average errors of 10 cm^{-1} (1.3 meV) for $\bar{\nu}_{11}$ and 40 cm^{-1} (5 meV) for $\bar{\nu}_{22}$. Compared to the previous fit with integer exponents, these expressions eliminate systematic fitting discrepancies and reduce average errors by approximately 70 and 40%. It seems likely that this accuracy will be retained on extrapolation to larger-diameter tubes, for which trigonal warping and curvature exert smaller spectral effects. Although extrapolation to smaller tube diameters is less secure, we expect the expressions to be useful down to ca. 0.5 nm.

Table 1 lists all 127 semiconducting nanotube structures having diameters between 0.48 and 2.00 nm (assuming a C−C distance of 0.144 nm) in order of increasing n and m values. Following the columns that show the diameter, chiral angle, and mod($n - m$, 3) values, we give the wavelengths, frequencies, and photon energies for first van Hove emission and second van Hove absorption as predicted by the equations above. Note that first van Hove absorption energies will be ca. 4 meV higher than the listed emission values.

In Figure 1, we plot the predicted and measured E_{11} and E_{22} values for semiconducting SWNT with diameters between 0.48 and 2.5 nm. A small set of measured values for E_{33} and E_{44} are also plotted. Empirical expressions for the energies of E_{33} and E_{44} transitions, which can also be important in resonance Raman studies of larger-diameter nanotubes, await further experimental measurements and analysis.

Discussion. Equations 1 and 2 are intended only as empirical fitting functions, and we do not suggest that the deduced parameters have any simple meaning within SWNT electronic structure models. Instead, the peculiar exponents deduced from fitting the data may reflect combinations of effects such as trigonal warping, curvature, and exciton binding.[10−14] Our fits and predictions apply to samples of individual SWNT in aqueous SDS suspension. Data measured by Lebedkin et al.[9] and in our laboratory suggest that small systematic spectral shifts of less than 2% can be

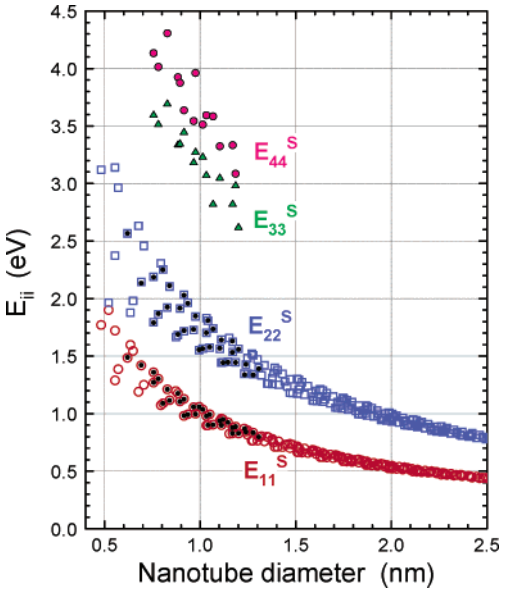

Figure 1. Optical transition energies vs diameter for semiconducting SWNT. Solid symbols are experimental data; open squares and circles are predictions of E_{11} and E_{22}, respectively, from the empirical fitting functions.

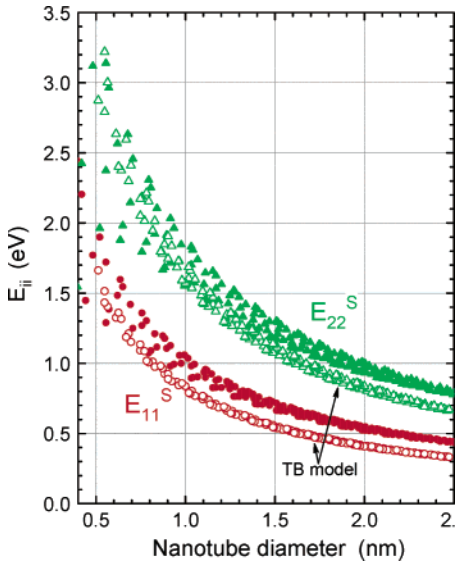

Figure 2. Comparison between model-based and empirical values of optical transition energies for semiconducting SWNT. Open symbols were computed using a simple tight binding (TB) model with $\gamma_0 = 2.90$ eV, and solid symbols were obtained from the empirically based fitting functions.

expected for individual SWNT suspended in other aqueous surfactants. Note, however, that our spectral fits are not applicable to bundled suspended nanotubes, for which strong perturbations between tubes lead to significantly broadened and red-shifted absorption spectra and quenched band-gap luminescence.[7]

Although Figure 1 qualitatively resembles model-based results, there are significant quantitative differences. To illustrate these, Figure 2 shows plots of E_{11} and E_{22} computed from a simple tight-binding model (as commonly used for Kataura plots) overlaid with the empirically based values from Figure 1. Both for E_{11} and E_{22} transitions, the tight-

binding model badly underestimates the apparent scatter arising from chiral variations at a given diameter. Empirically, these chiral variations in transition energy are at least twice as large as predicted by the tight-binding model for tube diameters of 1.5 nm or less. It is also clear that the tight-binding model (with $\gamma_0 = 2.90$ eV) underestimates E_{11} transition energies by up to 25% relative to the empirical values. Tight-binding E_{22} predictions are ca. 15% below the empirical values for 2.5-nm diameter tubes but as much as 25% *above* empirical values for some of the smallest-diameter species. Thus, adjusting γ_0 cannot bring the simple model predictions into accord with the empirically based transition energies. In our view, these deficiencies in model-based Kataura plots appear large enough to cause serious interpretation problems in some optical nanotube investigations. We therefore recommend that researchers performing optical experiments with surfactant suspensions of SWNT instead rely on the findings reported here to guide their work.

Acknowledgment. This research has been supported by the NSF (grants CHE-9900417 and CHE-0314270), the NSF Center for Biological and Environmental Nanotechnology (grant EEC-1008007), and the Robert A. Welch Foundation (grant C-0807). We thank the Carbon Nanotechnology Laboratory at Rice University for assistance in sample preparation and C. Kane for tight-binding model calculations.

Supporting Information Available: We present as Supporting Information a version of Table 1 extended to include nanotube structures through (25, 24) and the E_{ii} values measured to date in room-temperature aqueous SDS suspensions. This material is available free of charge via the Internet at http://pubs.acs.org.

References

(1) Saito, R.; Dresselhaus, G.; Dresselhaus, M. S. *Physical Properties of Carbon Nanotubes*; Imperial College Press: London, 1998.
(2) Hamada, N.; Sawada, S.; Oshiyama, A. *Phys. Rev. Lett.* **1992**, *68*, 1579−1581.
(3) Rao, A. M.; Richter, E.; Bandow, S.; Chase, B.; Eklund, P. C.; Williams, K. A.; Fang, S.; Subbaswamy, K. R.; Menon, M.; Thess, A.; Smalley, R. E.; Dresselhaus, G.; Dresselhaus, M. S. *Science* **1997**, *275*, 187−191.
(4) Dresselhaus, M. S.; Dresselhaus, G.; Jorio, A.; Souza Filho, A. G.; Pimenta, M. A.; Saito, R. *Acc. Chem. Res.* **2002**, *35*, 1070−1078.
(5) Kuzmany, H.; Plank, W.; Hulman, M.; Kramberger, Ch.; Gruneis, A.; Pichler, Th.; Peterlik, H.; Kataura, H.; Achiba, Y. *Eur. Phys. J. B* **2001**, *22*, 307−320.
(6) Kataura, H.; Kumazawa, Y.; Maniwa, Y.; Umezu, I.; Suzuki, S.; Ohtsuka, Y.; Achiba, Y. *Synth. Met.* **1999**, *103*, 2555−2558.
(7) O'Connell, M.; Bachilo, S. M.; Huffman, C. B.; Moore, V.; Strano, M. S.; Haroz, E.; Rialon, K.; Boul, P. J.; Noon, W. H.; Kittrell, C.; Ma, J.; Hauge, R. H.; Weisman, R. B.; Smalley, R. E. *Science* **2002**, *297*, 593−596.
(8) Bachilo, S. M.; Strano, M. S.; Kittrell, C.; Hauge, R. H.; Smalley, R. E.; Weisman, R. B. *Science* **2002**, *298*, 2361−2366.
(9) Lebedkin, S.; Hennrich, F. H.; Skipa, T.; Kappes, M. M. *J. Phys. Chem. B* **2003**, *107*, 1949−1956.
(10) Saito, R.; Dresselhaus, G.; Dresselhaus, M. S. *Phys. Rev. B* **2000**, *61*, 2981−2990.
(11) Reich, S.; Thomsen, C. *Phys. Rev. B* **2000**, *62*, 4273−4276.
(12) Ichida, M.; Mizuno, S.; Tani, Y.; Saito, Y.; Nakamura, A. *J. Phys. Soc. Jpn.* **1999**, *68*, 3131−3133.
(13) Ando, T. *J. Phys. Soc. Jpn.* **1997**, *66*, 1066−1073.
(14) Kane, C. L.; Mele, E. J. *Phys. Rev. Lett.* **2003**, *90*, 207401/1-4.

NL034428I